Received 22 October 2014
Revised 21 January 2015
Accepted 21 January 2015

Effects of saturation and hysteresis on magnetisation dynamics

Analysis of different material models

Martin Petrun
Faculty of Electrical Engineering and Computer Science, University of Maribor, Maribor, Slovenia
Simon Steentjes and Kay Hameyer
Institute of Electrical Machines, RWTH Aachen University, Aachen, Germany, and
Jožef Ritonja and Drago Dolinar
Faculty of Electrical Engineering and Computer Science, University of Maribor, Maribor, Slovenia

Abstract

Purpose – The purpose of this paper is to provide a comprehensive analysis of different material models when observing the magnetisation dynamics and power losses in non-oriented soft magnetic steel sheets (SMSSs).

Design/methodology/approach – During the analysis four different magnetic material models were used for describing the static material characteristics, which characterised the materials' magnetisation behaviour with increasing accuracies: linear material model, piecewise linear material model, non-linear *H(B)* characteristic and the static hysteresis material model proposed by Tellinen. The described material models were implemented within a parametric magneto-dynamic model (PMD) of SMSSs, where the dynamic responses as well as power loss calculations from the obtained models were analysed.

Findings – The momentous influences of various levels of detail on the calculation of dynamic variables and power losses inside SMSS with non-uniform magnetic fields were elaborated, where various static material characteristic models were evaluated, ranging from linear to hysteretic constitutive relationships.

Research limitations/implications – The resulting PMD model using different static models was analysed over a frequency range from quasi-static to $f = 1{,}000$ Hz for different levels of magnetic flux density up to $B_{\max} = 1.5$ T.

Practical implications – The presented analysis provides fundamental insight when calculating dynamic electromagnetic variables and power losses inside non-linear SMSSs, which is instrumental when selecting an adequate model for a specific application.

Originality/value – This paper provides closer insight on the way non-linearity, magnetic saturation and hysteresis affect the energy loss and magnetisation dynamics in SMSSs through the level of detail in the used material model. The strongly coupled model addresses both induced eddy currents and the ferromagnetic materials' magnetisation behaviour simultaneously using varying levels of detail so that the interplay between skin effect (i.e. eddy currents) across laminations and hysteresis can be resolved accurately. Therewith, adequate models for specific applications can be selected.

Keywords Magnetic hysteresis, Eddy currents, Skin effect, Power losses, Soft magnetic materials, Dynamic model

Paper type Research paper

COMPEL: The International Journal for Computation and Mathematics in Electrical and Electronic Engineering
Vol. 34 No. 3, 2015
pp. 710-723

0332-1649
DOI 10.1108/COMPEL-10-2014-0286

The work of M. Petrun was supported by the Slovenian Research Agency (ARRS), Project Numbers P2-0115, L2-5489 and L2-4114. The work of S. Steentjes was supported by the Deutsche Forschungsgemeinschaft (DFG) as part of the research project "Improved modeling and characterization of ferromagnetic materials and their losses".

I. Introduction

The magnetisation dynamics in long and thin non-oriented (NO) soft magnetic steel sheets (SMSS) with predominately small domains are adequately described in many cases using 1D quasi-static approximation of the magnetic phenomena inside the SMSS (Zirka *et al.*, 2006, 2008). Such approximation can be obtained using various methods and models, where, e.g. FD- or FE-coupled models (Zirka *et al.*, 2006, 2008; Bottauscio *et al.*, 2004), magnetic equivalent circuits (Bottauscio *et al.*, 2004; Hui *et al.*, 1996) and more recently the parametric magneto-dynamic (PMD) model (Petrun *et al.*, 2014a, b) represent established non-linear dynamic models. The 1D approximation is also extended in some cases for the calculations of 2D (Belahcen *et al.*, 2014) and 3D models (Cheng *et al.*, 2013). Alternative approaches for use in engineering often also represent various simplified descriptions for loss calculations. These are e.g., based on empirical approaches derived from the Steinmetz equation (Novak *et al.*, 2014) or based on analytical calculations (Wang *et al.*, 2014; Raminosoa *et al.*, 2014), where linear material properties with momentous and treacherous limitations are often considered. Such models are based on strong simplistic assumptions that profoundly ease the intricate magnetic material's behaviour and have as a result limited accuracy and usability (Beatrice *et al.*, 2014). As seen in the literature (Bottauscio *et al.*, 2002; Rasilo *et al.*, 2011), the used material model can have significant influences on the calculated accuracies of the dynamic electromagnetic variables and power loss components.

The objective of this paper was therefore to analyse the effects of different static material models on the behaviour and accuracies of the calculated magnetisation dynamics and power loss components inside discussed SMSSs. For this purpose the PMD model (Petrun *et al.*, 2014a, b) was coupled with four different static material models. The coupled models were evaluated over a wide-range from quasi-static to $f = 1{,}000$ Hz at different magnetic flux density levels up to $B_{max} = 1.5$ T, where the effects of saturation, non-linearity and magnetic hysteresis regarding dynamic magnetisation and power losses were studied. The presented systematic analysis provides fundamental insight when calculating dynamic electromagnetic variables and losses inside non-linear SMSSs, which is instrumental when selecting an adequate model for a specific application.

II. Theoretical background

A. PMD model of SMSSs

Using the PMD model, the magnetic field distribution inside a SMSS is described piecewise uniformly across the SMSS thickness by dividing the SMSS into several slices s. The magnetic fields inside individual slices can be treated as uniform when the SMSS is divided into an adequate number of slices N_s, where the first slice ($s = 1$) is assumed to be in the centre and last slice ($s = N_s$) close to the surface of the SMSS (Petrun *et al.*, 2014a, b). The magnetic field inside the SMSS is described using a system of differential equations for all slices s in matrix form (1), where $\mathbf{N} = N[1]_{Ns\times 1}$ represents a vector composed of excitation winding turns N, i being the current in the excitation winding, $\overline{\mathbf{H}}(\overline{\mathbf{\Phi}})$ a vector of magnetic field strengths such as linear, piecewise linear, non-linear or hysteretic functions of the average magnetic fluxes of individual slices, l_m the mean magnetic path length and $\mathbf{L}_m$ representing the so-called magnetic inductance matrix of the SMSS:

$$\mathbf{N}i = \overline{\mathbf{H}}(\overline{\mathbf{\Phi}})l_m + \mathbf{L}_m \frac{d\overline{\mathbf{\Phi}}}{dt} \quad (1)$$

The matrix of magnetic inductance $\mathbf{L}_\mathrm{m}$ is defined by (2) and depends on the geometric and material properties as well as on the discretisation of the observed SMSS, where b is the thickness, a is the width, A_Fe is the effective cross-section and σ is the specific electric conductivity of the SMSS. The dimensions of the matrix of magnetic inductance $\mathbf{L}_\mathrm{m}$ depend on the discretisation of the SMSS, i.e. the number of slices N_s:

$$\mathbf{L}_\mathrm{m} = \sigma l_\mathrm{m}\left(\frac{b}{2N_\mathrm{s}}\right)^2\left(\frac{N_\mathrm{s}}{A_\mathrm{Fe}}\right)\begin{bmatrix} (N_\mathrm{s}-1)+\frac{1}{3} & (N_\mathrm{s}-2)+\frac{1}{2} & \cdots & 1+\frac{1}{2} & \frac{1}{2} \\ (N_\mathrm{s}-2)+\frac{1}{2} & (N_\mathrm{s}-2)+\frac{1}{3} & \cdots & 1+\frac{1}{2} & \frac{1}{2} \\ \vdots & \vdots & \ddots & \vdots & \vdots \\ 1+\frac{1}{2} & 1+\frac{1}{2} & \cdots & 1+\frac{1}{3} & \frac{1}{2} \\ \frac{1}{2} & \frac{1}{2} & \cdots & \frac{1}{2} & \frac{1}{3} \end{bmatrix}_{N_\mathrm{S}\times N_\mathrm{S}} \quad (2)$$

The number of slices N_s can be adapted according to the excitation dynamics and material properties, which also define the penetration depth of the magnetic field. When applying lower excitation dynamics, division into fewer slices is required as the magnetic field inside the SMSS is more uniform. For higher excitation dynamics the number of slices N_s should be increased to adequately describe the non-uniform magnetic field inside the observed SMSS. Adequate discretisation can be obtained e.g., following the guidelines presented in Hui *et al.* (1996).

The electromagnetic variables inside the SMSS can be calculated based either on the excitation current i, or based on the applied voltage u on the excitation winding. For the voltage-driven excitation case an additional equation is needed, where the induced voltage u_i in the excitation winding is taken into account. The calculation of induced voltage is based on the average magnetic flux Φ_m inside the SMSS (3), where $\overline{\boldsymbol{\Phi}}$ represents a vector of average values of magnetic fluxes inside individual slices within the SMSS:

$$u_\mathrm{i} = -N\frac{\mathrm{d}\Phi_\mathrm{m}(\Theta)}{\mathrm{d}t} = -\mathbf{N}^\mathrm{T}\frac{\mathrm{d}\overline{\boldsymbol{\Phi}}}{\mathrm{d}t} \quad (3)$$

B. Static magnetic constitutive relationships

The relationships $H(B)$ used to describe the static magnetisation behaviour (1) inside individual slices s can be calculated using different material models. In this work four different material models with increasing accuracies were implemented and evaluated:

(1) linear, purely reversible material model, where $H(B) = B/(\mu_0\mu_\mathrm{r})$ with $\mu_\mathrm{r} = 8{,}000$;

(2) piecewise linear (PWL) material model based on a linear model including a saturation region with $\mu_\mathrm{r} = 1$;

(3) non-linear $H(B)$ characteristic based on measurements, i.e., measured initial magnetisation curve; and

(4) the static hysteresis model proposed by Tellinen (1998), based on measurements.

All four used static magnetic material descriptions are shown and compared in Figure 1.

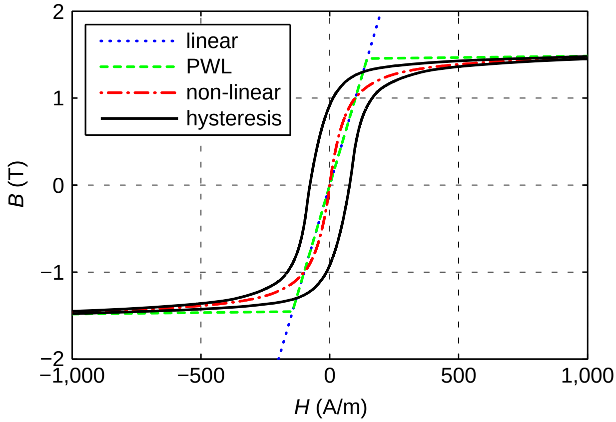

Figure 1. Comparisons between used material models

C. Power loss calculation

According to Petrun *et al.* (2014b), the instantaneous conduction power loss $p_{es}(t)$ due to eddy currents within each slice is calculated by (4). Furthermore, instantaneous powers $p_{hs}(t)$ due to the static hysteresis effects inside slices are calculated by (5), where the calculation procedure of $p_{hs}(t)$ is independent of the applied hysteresis model:

$$p_{es} = 2\sigma a l_m b_s^3 \left[\left(\sum_{i=1}^{s-1} \frac{d\overline{B}_i}{dt} \right)^2 + \left(\sum_{i=1}^{s-1} \frac{d\overline{B}_i}{dt} \right) \frac{d\overline{B}_s}{dt} + \frac{1}{3} \left(\frac{d\overline{B}_s}{dt} \right)^2 \right] \quad (4)$$

$$p_{hs} = a b_s l_m \overline{H}_s \frac{d\overline{B}_s}{dt} \quad (5)$$

Using (4) and (5) energies W_{es} and W_{hs} and average powers P_{es} and P_{hs} within an arbitrary observed time period $\Delta t = (t_2 - t_1)$ inside individual slice s are calculated by (6) and (7):

$$P_{es} = \frac{W_{es}}{\Delta t} = \frac{1}{\Delta t} \int_{t_1}^{t_2} p_{es}(t) dt, \quad (6)$$

$$P_{hs} = \frac{W_{hs}}{\Delta t} = \frac{1}{\Delta t} \int_{t_1}^{t_2} p_{hs}(t) dt, \quad (7)$$

The total instantaneous powers p_e and p_h, energies W_e and $W_{h,}$ and the average powers P_e and P_h for the entire SMSS are obtained by summing the components of the individual slices. When fully reversible material models are applied, the hysteresis loss component is neglected, hence the calculated average powers P_{hs} within a characteristic time period Δt amount to $P_{hs} = 0$.

III. Results

The discussed four coupled models were evaluated by comparing calculated and measured major and symmetrical minor dynamic hysteresis loops for a M400-50A NO steel (Table I) using sinusoidal excitation. The experimental results for the presented evaluation were carried out on an Epstein frame, which was incorporated within a computer-aided set-up in accordance with the international standard IEC 60404-2. The SMSS sample was characterised using controlled sinusoidal magnetic flux density with a form-factor error of less than 1 per cent within the frequency range from quasi-static to 1,000 Hz. The static material models were characterised and parameterised using quasi-static measurement results for the M400-50A NO steel, where the relative permeability $\mu_r = 8{,}000$ for the linear case was determined in such a way that the linear characteristic crossed the non-linear characteristic at $B = 1$ T (Figure 1).

Dynamic magnetisations were calculated by dividing the SMSS into ten slices ($N_s = 10$). Figures 2-4 show comparisons between magnetisation dynamics in the PMD model when using different static material models for excitation frequency $f = 1{,}000$ Hz and maximum average flux densities $B_{max} = 1.5$ T, $B_{max} = 1.0$ T and $B_{max} = 0.5$ T, respectively. The obtained results showed significant differences when using the discussed material models, with the more significant deviations at $B_{max} = 1.5$ T (Figure 2), where the whole SMSS reached saturation. When using the linear static material model in such a case (Figure 2(a)), the calculated results showed non-physical behaviour with too high skin effect as the magnetic flux density in the outer slice ($s = 10$) reached almost 4 T. Con*s*equently the shape of the calculated dynamic hysteresis loop also deviated heavily from the measured hysteresis loop.

A significantly increased level of detail was obtained regarding the magnetisation behaviour when applying the piecewise linear material model with a step-like magnetisation curve (Figure 2(b)). Although the calculated dynamic variables showed abrupt changes when individual slices reached saturation, the obtained dynamic hysteresis showed strong resemblance to the measured one. The next improvement was achieved if the non-linear material model were to be applied (Figure 2(c)). In such a case the aforementioned abrupt changes were eliminated, which was visible in the time behaviour of the magnetic flux densities B_s as well as in the induced eddy currents i_{es} inside individual slices of the SMSS. When comparing the measured and calculated dynamic hysteresis loops it was visible that the calculated loops had good shape agreement, however the latter hysteresis was narrower than the former. This deviation occurred because a purely reversible non-linear material model was used, where the hysteresis losses were neglected, thus only eddy current losses were calculated. As seen in Figure 2(d), this difference can be eliminated using an adequate hysteresis model, where the hysteresis losses are taken into account. In such a case the best accordance between measured and calculated dynamic hysteresis loops is obtained. An obvious skin effect was apparent using the linear material model (Figure 2(a)) but there was in

Table I.
M400-50A
NO SMSS data

Parameter	Quantity	Value
A_{Fe}	Effective cross-section of the SMSS	15 mm^2
l_m	Mean magnetic path length of the SMSS	940 mm
b	Thickness of the SMSS	0.5 mm
a	Width of the SMSS	30 mm
σ	Specific electric conductivity of the SMSS	2.2×10^6 S/m

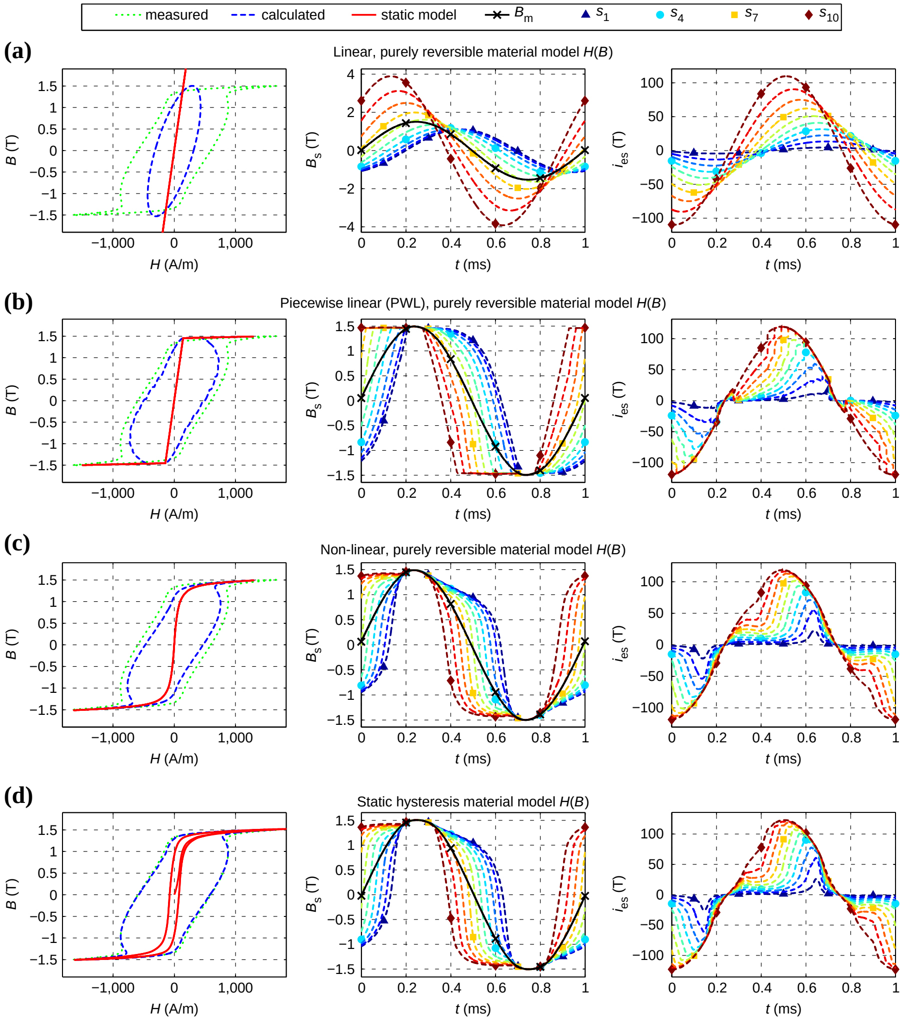

Notes: First row, linear $H(B)$ characteristic; second row, piecewise linear $H(B)$ characteristic including saturation, third row, non-linear $H(B)$ characteristic; and fourth row, hysteretic $H(B)$ characteristic. First column shows the comparison between the measured and calculated dynamic hysteresis loops and used static $H(B)$ characteristic, whereas the second and third columns show corresponding flux densities B_s and eddy currents i_{es} in all ten slices of the SMSS

Figure 2. Comparisons between the influences of different material models on magnetisation dynamics in a M400-50A NO SMSS for $f = 1{,}000$ Hz and $B_{max} = 1.5$ T

fact almost no difference between the magnetic flux density peaks at different sheet depths using the other material models (Figure 2(b)-(c)), which consider material saturation.

The differences between the four used models become significantly smaller when comparing the calculated results at lower maximum average flux densities B_{max}. At $B_{max} = 1.0$ T (Figure 3) only the outer slices reach saturation due to skin effect and consequently the deviations between the reversible material models (Figure 3(a)-(c))

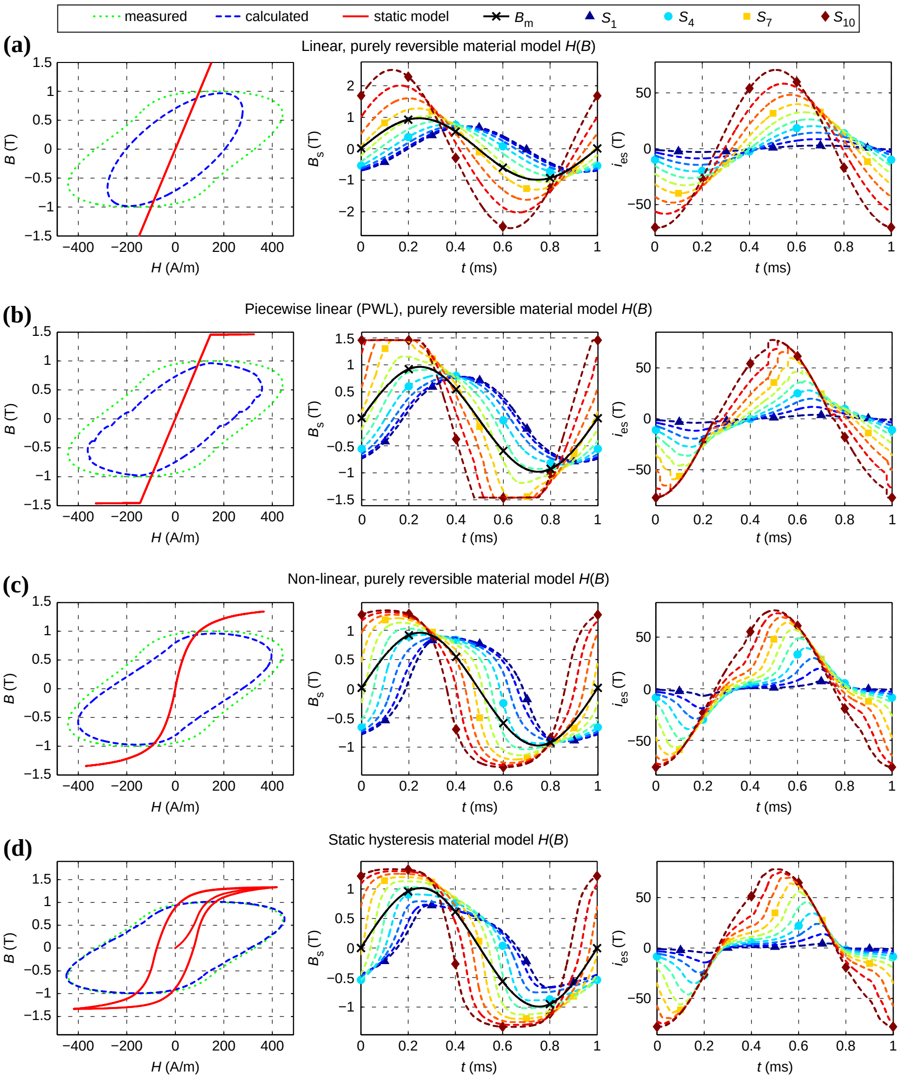

Figure 3. Comparisons between the influence of different materials' models on magnetisation dynamics in a M400-50A NO SMSS for $f = 1{,}000$ Hz and $B_{max} = 1$ T

Notes: First row, linear $H(B)$ characteristic; second row, piecewise linear $H(B)$ characteristic including saturation, third row, non-linear $H(B)$ characteristic; and fourth row, hysteretic $H(B)$ characteristic. First column shows the comparison between the measured and calculated dynamic hysteresis loops and used static $H(B)$ characteristic, whereas the second and third columns show corresponding flux densities B_s and eddy currents i_{es} in all ten slices of the SMSS

became smaller. However, in this case also the importance of the saturation effect was clearly visible. The material saturation influenced the loop-shape of the dynamic hysteresis even if only a part of the SMSS was saturated. As in the previous case the best match between the measured and calculated loop shapes was obtained when using

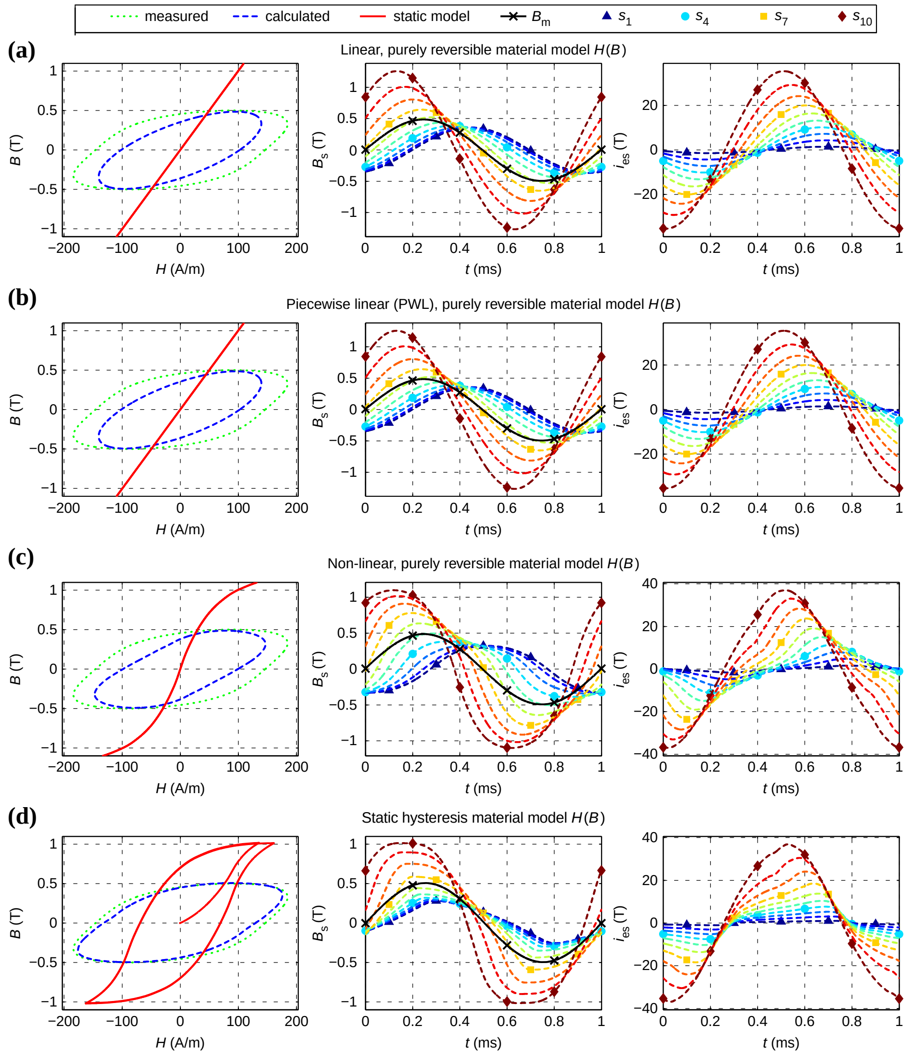

Notes: First row, linear $H(B)$ characteristic; second row, piecewise linear $H(B)$ characteristic including saturation; third row, non-linear $H(B)$ characteristic; and fourth row, hysteretic $H(B)$ characteristic. First column shows the comparison between the measured and calculated dynamic hysteresis loops and used static $H(B)$ characteristic, whereas the second and third columns show corresponding flux densities B_s and eddy currents i_{es} in all ten slices of the SMSS

Figure 4. Comparisons between the influences of different materials' models on magnetisation dynamics in a M400-50A NO SMSS for $f = 1{,}000$ Hz and $B_{max} = 0.5$ T

the static hysteresis material model. In all four models an obvious skin effect was present at this average magnetic flux density, which underlines the need for considering this non-linear skin effect behaviour (compare Figures 2 and 3).

When comparing the discussed models at low maximum average flux densities B_{max}, where the observed SMSS is not saturated, the differences between the reversible materials' models (Figure 4(a)-(c)) almost vanished. At $B_{max} = 0.5$ T (Figure 4) there was no difference between the linear and PWL cases (Figures 4(a) and (b)) as saturation inside the observed SMSS was not reached. A small difference was obtained using the non-linear model (Figure 4(c)) due to the non-linearity of the relative permeability. The best results were obtained using the static hysteresis description. From the gathered results it can be concluded that at low maximum flux densities, where the saturation is not reached, the eddy current losses could be approximated using a linear material model.

Deeper insight can be obtained when comparing the calculated power losses using the discussed material models. Figure 5 shows the comparisons between the measured and calculated power loss components where two characteristic cases are evaluated. It is interesting that at lower excitation frequencies (e.g. $f = 200$ Hz, Figure 5(a)) there was almost no significant difference between the calculated eddy current losses P_e when using all four material models. In contrast to this significant differences between calculated P_e occurred at higher frequencies (e.g. $f = 1{,}000$ Hz, Figure 5(b)), where the highest deviation was obtained using the linear material model. Furthermore, as already concluded from Figures 2-4, the deviation of the linear model increased with increased maximum average flux densities B_{max}, where the effect of saturation significantly affected the calculated results (Zirka *et al.*, 2010).

The good agreements at lower excitation frequencies (e.g. $f = 200$ Hz, Figure 5(a) between all the used models were, however, very instructive. Surprisingly the deviation of the linear model was insignificant even at higher maximum flux densities B_{max}, where the SMSS was already saturated. The explanation for the obtained results could be achieved when the skin depths for both excitation cases were calculated for $\mu_r = 8{,}000$. For the frequency $f = 200$ Hz the skin depth is approximately 0.27 mm, whereas the skin depth for the frequency $f = 1{,}000$ Hz is approximately 0.12 mm. The thickness of the observed SMSS was 0.5 mm, which implied that the magnetic field inside the SMSS at $f = 200$ Hz could be considered as almost uniform, whereas the magnetic field inside the SMSS was highly non-uniform at $f = 1{,}000$ Hz. Hence it can be concluded that the eddy current losses P_e can be estimated with sufficient precision

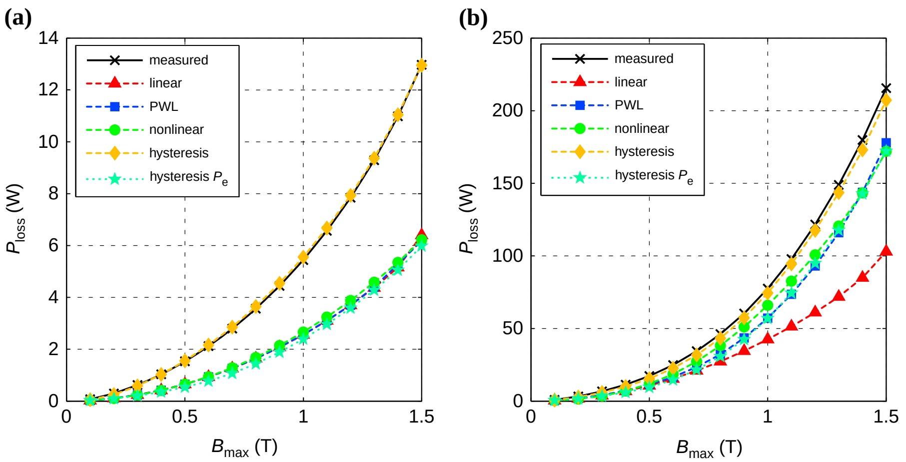

Notes: (a) f = 200 Hz and (b) f = 1,000 Hz

Figure 5.
Comparisons between measured and calculated power loss components

using all four material models, when the excitation frequency is adequately low so that the skin depth is higher than half the thickness of the SMSS. However, it should be noted that the results of the linear and piecewise linear models strongly depended on the parameterisation, i.e., the relative permeability μ_r and the knee-point where the saturation region started.

The small deviation in the calculated eddy current losses was further investigated by comparing the dynamic hysteresis loops using linear and non-linear material models at $f = 200$ Hz (Figure 6(a) and $f = 1{,}000$ Hz (Figure 6(b)). From the obtained results it was visible that in the cases of almost uniform magnetic fields (Figure 6(a)) the deviations between the linear and non-linear cases only occurred when the SMSS approached saturation. The calculated dynamic variables showed significant deviation in this part, the surfaces of both hysteresis loops were, however very similar, hence the calculated losses also agreed very well.

In the case of non-uniform magnetic fields (Figure 6(b)) the magnetic fields inside the SMSS approached saturation progressively, where the outer slices approached saturation first. Due to this phenomenon the calculated dynamic hysteresis loop was flattened and inflated with a characteristic "belly". Due to the effects of non-linearity and non-uniform magnetic fields inside the SMSS the calculated results obtained using the linear material models were inadequate.

The calculation of eddy current losses P_e using the three reversible materials' models were further evaluated vs frequency at different maximum flux densities (Figure 7). From the obtained results it could be examined that the deviations between different models were smaller at low maximum flux densities (e.g. $B_{max} = 0.5$ T, Figure 7(a)), where the SMSS is not saturated. In this case the deviations started to increase with increasing excitation frequencies, as the skin effect increased and the magnetic fields started to approach saturation. At higher maximum flux densities (e.g. $B_{max} = 1.5$ T, Figure 7(c)) the effect of saturation increased the calculated eddy current losses. Consequently the calculated results using the linear model were inadequate when the magnetic fields inside the SMSS were non-uniform. The linear material model can be applied at excitation frequencies where skin depth is higher than half the thickness of the SMSS ($f < 200$ Hz, Figure 7(c)).

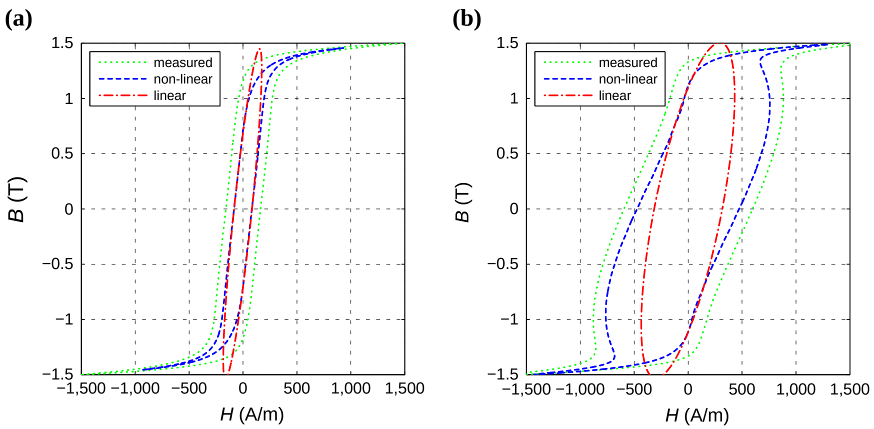

Notes: (a) f = 200 Hz; (b) f = 1,000 Hz

Figure 6. Comparisons between the calculated dynamic hysteresis using linear and non-linear material models

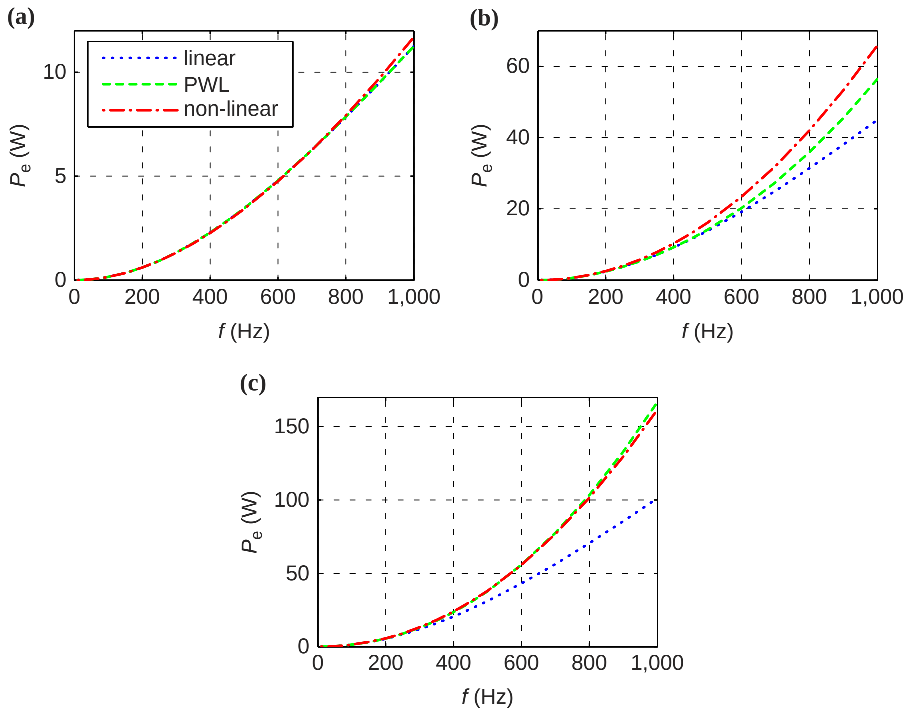

Notes: (a) B_{max} = 0.5 T; (b) B_{max} = 1 T; (c) B_{max} = 1.5 T

Figure 7. Comparisons between the calculated power loss components using different materials' models

IV. Conclusion

The presented paper analysed the effects of material saturation and magnetic hysteresis on magnetisation dynamics in NO SMSSs. In the paper the importance of accounting for non-linear properties and saturation when calculating dynamic variables and power losses inside SMSS with non-uniform magnetic fields was pointed out. Due to non-linear properties the amplitude differences and phase shifts between the magnetic fields inside individual slices of the SMSS were significantly decreased, as well as eddy current power losses being significantly increased, especially at high excitation dynamics and magnetic flux density levels. Simplified linear materials' properties can be applied only for eddy current power loss estimation at sufficiently low excitation frequencies and magnetic flux density levels. However such simplification is inadequate when calculating dynamic electromagnetic variables. Using adequate static hysteresis models coupled with the SMSS model is instrumental when calculating dynamic behaviour and power loss components over wide frequency ranges, as at low frequencies the power losses are dominated by hysteresis effects, hence the reversible models are not adequate enough. At higher frequencies the power losses are dominated by eddy currents, however the use of the linear material model is inappropriate. At very high frequencies, where the hysteresis losses could be neglected in comparison to the eddy current losses, the non-linear, fully reversible material model could be applied to achieve sufficient accuracy.

The presented analysis provides fundamental insight when calculating dynamic electromagnetic variables and power losses inside non-linear SMSSs, which is instrumental when selecting an adequate model for a specific application. The future work will focus on analysis when applying different material models when modelling grain-oriented SMSSs with significantly different domain structures and strongly anisotropic magnetic behaviour (Baghel and Kulkarni, 2013). Furthermore, the influences of the uncertainties introduced on the soft magnetic material properties during the manufacturing process (Ramarotafika *et al.*, 2012) on the magneto-dynamic properties for arbitrary magnetisation waveforms, could be also investigated in detail using the presented PMD model.

References

Baghel, A.P.S. and Kulkarni, S.V. (2013), "Hysteresis modeling of the grain-oriented laminations with inclusion of crystalline and textured structure in a modified Jiles-Atherton model", *Journal of Applied Physics*, Vol. 113 No. 4, pp. 043908-043908-5.

Beatrice, C., Appino, C., de la Barrière, O., Fiorillo, F. and Ragusa, C. (2014), "Broadband magnetic losses in Fe-Si and Fe-Co laminations", *IEEE Transactions On Magnetics*, Vol. 50 No. 4, pp. 1-4.

Belahcen, A., Rasilo, P. and Arkkio, A. (2014), "Segregation of iron losses from rotational field measurements and application to electrical machine", *IEEE Transactions On Magnetics*, Vol. 50 No. 2, pp. 893-896.

Bottauscio, O., Canova, A., Chiampi, M. and Repetto, M. (2002), "Iron losses in electrical machines: influence of different material models", *IEEE Transactions On Magnetics*, Vol. 38 No. 2, pp. 805-808.

Bottauscio, O., Manzin, A., Canova, A., Chiampi, M., Gruosso, G. and Repetto, M. (2004), "Field and circuit approaches for diffusion phenomena in magnetic cores", *IEEE Transactions On Magnetics*, Vol. 40 No. 2, pp. 1322-1325.

Cheng, L., Sudo S., Gao, Y., Dozono, H. and Muramatsu, K. (2013), "Homogenization technique of laminated core taking account of eddy currents under rotational flux without edge effect", *IEEE Transactions On Magnetics*, Vol. 49 No. 5, pp. 1969-1972.

Hui, S.Y.R., Zhu, J.G. and Ramsden, V.S. (1996), "A Generalized dynamic circuit model of magnetic cores for low- and high-frequency applications – part II: circuit model formulation and implementation", *IEEE Transactions On Power Electronics*, Vol. 11 No. 2, pp. 251-259.

Novak, G., Kokosar, J., Nagode, A. and Steiner Petrovic, D. (2014), "Core-loss prediction for non-oriented electrical steels based on the steinmetz equation using fixed coefficients with a wide frequency range of validity", *IEEE Transactions On Magnetics*, Vol. PP No. 99, p. 1.

Petrun, M., Podlogar, V., Steentjes, S., Hameyer, K. and Dolinar, D. (2014a), "A Parametric magneto-dynamic model of soft magnetic steel sheets", *IEEE Transactions On Magnetics*, Vol. 50 No. 4, pp. 1-4.

Petrun, M., Podlogar, V., Steentjes, S., Hameyer, K. and Dolinar, D. (2014b), "Power loss calculation using the parametric magneto-dynamic model of soft magnetic steel sheets", *IEEE Transactions On Magnetics*, Vol. 50 No. 11, pp. 1-4.

Ramarotafika, R., Benabou, A. and Clenet, S. (2012), "Stochastic modeling of soft magnetic properties of electrical steels: application to stators of electrical machines", *IEEE Transactions On Magnetics*, Vol. 48 No. 10, pp. 2573-2584.

Raminosoa, A.T., Chillet, C., Fassenet, M., Yonnet, J. and Voyant, J. (2014), "An analytical approach of magnetic diffusion in a plate under time-varying flux excitation", *IEEE Transactions On Magnetics*, Vol. 50 No. 4, pp. 1-11.

Rasilo, P., Dlala, E., Fonteyn, K., Pippuri, J., Belahcen, A. and Arkkio, A. (2011), "Model of laminated ferromagnetic cores for loss prediction in electrical machines", *IET Electric Power Applications*, Vol. 5 No. 7, pp. 580-588.

Tellinen J. (1998), "A simple scalar model for magnetic hysteresis", *IEEE Transactions On Magnetics*, Vol. 34 No. 4, pp. 2200-2206.

Wang, J., Lin, H., Li, H., Fang, S., Huang, Y. Dong, J. and Hui, Y. (2014), "Linear representation of saturation characteristics associated with eddy currents in ferromagnetic materials", *IEEE Transactions On Magnetics*, Vol. 50 No. 2, pp. 121-124.

Zirka, S.E., Moroz, Y.I., Marketos, P. and Moses, A.J. (2006), "Viscosity-based magnetodynamic model of soft magnetic materials", *IEEE Transactions On Magnetics*, Vol. 42 No. 9, pp. 2121-2132.

Zirka, S.E., Moroz, Y.I., Marketos, P. and Moses, A.J. (2010), "Loss separation in non-oriented electrical steels", *IEEE Transactions On Magnetics*, Vol. 46 No. 2, pp. 286-289.

Zirka, S.E., Moroz, Y.I., Marketos, P., Moses, A.J., Jiles, D.C. and Matsuo, T. (2008), "Generalization of the classical method for calculating dynamic hysteresis loops in grain-oriented electrical steels", *IEEE Transactions On Magnetics*, Vol. 44 No. 9, pp. 2113-2126.

About the authors

Dr Martin Petrun received his BSc and PhD in Electrical Engineering from the University of Maribor, Maribor, Slovenia, in 2010 and 2014, respectively. He is currently working as a Researcher and an Assistant Professor at the University of Maribor. His current research interests include modelling of dynamic phenomena inside soft magnetic materials as well as modelling and control of electrical and electromechanical converters and power electronics. Dr Martin Petrun is the corresponding author and can be contacted at: martin.petrun@um.si

Simon Steentjes received his Diploma degree in Electrical Engineering from the RWTH Aachen University, Germany, in November 2011. He has been working as a Research Associate at the Institute of Electrical Machines since December 2011. His research interests include hard- and soft magnetic material modelling on the micro- and macroscopic scale, iron loss calculation, effects of material processing, magnetic forces and mathematical methods.

Professor Kay Hameyer received his MSc in the Electrical Engineering from the University of Hannover and his PhD from the Berlin University of Technology, Germany. After his university studies he worked with the Robert Bosch GmbH in Stuttgart, Germany as a Design Engineer for permanent magnet servo motors and vehicle board net components. Until 2004 Dr Hameyer was a Full Professor for Numerical Field Computations and Electrical Machines with KU Leuven in Belgium. Since 2004, he has been a Full Professor and the Director of the Institute of Electrical Machines (IEM) at RWTH Aachen University in Germany. In 2006 he was the Vice Dean of the faculty and from 2007 to 2009 was the Dean of the Faculty of Electrical Engineering and Information Technology of RWTH Aachen University. His research interests are numerical field computation and optimisation, the design and controls of electrical machines, in particular permanent magnet excited machines, induction machines and design employing the methodology of virtual reality. Since several years Dr Hameyer's work is concerned with the magnetic levitation for drive systems, magnetically excited audible noise in electrical machines and the characterisation of ferromagnetic materials. Dr Hameyer is author of more than 250 journal publications, more than 500 international conference publications and author of four books. Dr Hameyer is a member of VDE, IEEE senior member, fellow of the IET.

Dr Jožef Ritonja was born in Maribor, Slovenia in 1964. He received his BSc, MSc and PhD degrees in Electrical Engineering from the University of Maribor, Maribor, Slovenia, in 1986, 1989 and 1996, respectively. Since 1987 he has been working at the University of Maribor, Faculty of Electrical Engineering and Computer Science in the field of control theory, electrical machines and power systems.

Professor Drago Dolinar received his BSc, MSc, and PhD in Electrical Engineering from the University of Maribor, Maribor, Slovenia, in 1978, 1980 and 1985, respectively. Since 1981, he has been with the Faculty of Electrical Engineering and Computer Science of the University of Maribor where he is currently a Professor. His current research interests include modelling and control of electrical machines. Dr Dolinar is a member of the Institution of Engineering and Technology (IET), IEEE, ICS, the Conseil International des Grands Reseaux Electriques (CIGRÉ), and the Slovenian Simulation Society (SloSim).